Interference of Coherent Polariton Beams in Microcavities: Polarization-Controlled Optical Gates

C. Leyder,[1] T. C. H. Liew,[2] A. V. Kavokin,[2] I. A. Shelykh,[3,4] M. Romanelli,[1] J. Ph. Karr,[1,5] E. Giacobino,[1] and A. Bramati[1]

[1]*Laboratoire Kastler Brossel, Université Paris 6, Ecole Normale Supérieure et CNRS, UPMC Case 74, 4 place Jussieu, 75252 Paris Cedex 05, France*

[2]*School of Physics and Astronomy, University of Southampton, Highfield, Southampton SO17 1BJ, United Kingdom*

[3]*International Center for Condensed Matter Physics, Universidade de Brasilia, 70904-970, Brasilia-DF, Brazil*

[4]*St. Petersburg State Polytechnical University, 195251, St. Petersburg, Russia*

[5]*Departement de Physique et Modelisation, Universite d'Evry Val d'Essonne, Boulevard F. Mitterrand, 91025 Evry, France*

(Received 2 February 2007; published 7 November 2007)

We demonstrate, theoretically and experimentally, a polarization-controlled optical gate based on a degenerate polariton-polariton scattering process occurring in semiconductor microcavities. Because of the interference between coherent polaritons, this process is observed in the case of polaritons generated from two collinearly polarized coherent pump beams. On the contrary, if the beams are cross polarized, the scattering is suppressed.

DOI: 10.1103/PhysRevLett.99.196402 PACS numbers: 71.36.+c, 03.75.Kk, 42.65.−k

Introduction.—Coherent quantum effects in many body systems open the way to many novel applications including the measurement of atomic refractive index using Ramsey fringes [1] and the construction of quantum logic gates [2]. Aside from being the signature of the wavelike nature of matter, the interference is a powerful tool for studying the properties of material systems such as excitons in quantum wells [3]. With the recent experimental confirmation of Bose-Einstein condensation in semiconductor microcavities [4], the use of interference of coherent matter states to construct new devices becomes a real possibility. We report the construction of one such device that functions as an optical gate.

Typical optical gates rely on material nonlinearities to function; changes in the refractive index of a material caused by one light beam can be used to modulate the intensity of another. However, nonlinear coefficients in materials are generally small and many designs require high powers to function. In recent years, resonant-enhanced nonlinear effects in photonic crystals [5] and micro-ring resonators [6–8] have been used to increase signal intensities by several orders of magnitude. We show that by exploiting the correlation and interference effects in polariton-polariton scattering in microcavities, one can create optical gates that could have shorter response times and lower thresholds than existing devices.

In semiconductor microcavities the coherent exchange of energy between excitons and photons can be described in terms of half-matter half-light bosonic quasiparticles named polaritons [9,10]. Polaritons are easily created and detected through the capture and escape of photons in and out of the microcavity. Coulomb interactions between the excitonic components allow polaritons to scatter elastically with one another [11,12]. Very recently, it was shown that these interactions allow a process [13] in which two degenerate, continuous wave (cw) lasers pump resonantly the lower polariton branch at opposite wave vectors and give rise to a strong signal in opposite directions on an elastic circle [illustrated in Fig. 1(a)]. The signal beams were shown to be well correlated in intensity. The effect is unexpected from classical arguments of energy-momentum conservation alone, which were able to qualitatively explain the angular distribution of scattered polaritons in a similar pumping scheme [14]. Indeed, all the scattering trajectories shown in Fig. 1(b) are equally allowed by energy-momentum conservation laws and the scattering matrix element can be assumed wave vector independent to a good accuracy [15–18]. Rather, the comprehension of this symmetry breaking of scattered polaritons requires a theory that takes into account the wave nature of interacting polaritons. In this Letter we present such a theory, which also accounts for the polarization degree of freedom of polaritons. We show that the scattering of polaritons is governed by the relative polarization of the two pumps, so

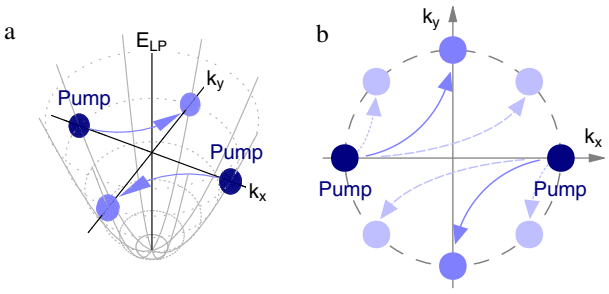

FIG. 1 (color online). Illustration of elastic scattering between two polaritons generated resonantly by pumps with equal and opposite wave vector. (a) The polariton dispersion; (b) the elastic circle in reciprocal space. Instead of being scattered uniformly around the elastic circle, as indicated by the lightest spots in (b), the theory predicts a preferential scattering to the wave vectors perpendicular to the pumps.

that a polarization-controlled optical gate of a micron size can be realized. Our theoretical predictions are confirmed by new experimental results.

Theoretical model.—Polaritons are composite bosons and have two allowed spin projections on the axis of the cavity. Their polarization (linear, circular, or elliptical) is fully described by a 3D vector called *pseudospin* [15]. A coherent ensemble of polaritons is described by two coupled wave functions, $\vec{\chi}(\vec{x})$ and $\vec{\phi}(\vec{x})$, which represent excitons and photons in a microcavity, respectively. Each wave function is a vector with two components representing two orthogonal linear polarizations (say, x and y). Polariton-polariton interactions are accounted for using the zero-range interaction and mean-field approximations that lead to the Gross-Pitaevskii equations [18], which describe wave function evolution:

$$i\hbar\frac{\partial\vec{\chi}(\vec{x})}{\partial t} = -\frac{\hbar^2\nabla^2}{2m_\chi}\vec{\chi}(\vec{x}) + \Omega\vec{\phi}(\vec{x}) + V_0[\vec{\chi}^*(\vec{x})\cdot\vec{\chi}(\vec{x})]\vec{\chi}(\vec{x}) - V_1\vec{\chi}^*(\vec{x})[\vec{\chi}(\vec{x})\cdot\vec{\chi}(\vec{x})] - \frac{i\hbar}{2\tau_\chi}\vec{\chi}(\vec{x}), \quad (1)$$

$$i\hbar\frac{\partial\vec{\phi}(\vec{x})}{\partial t} = -\frac{\hbar^2\nabla^2}{2m_\phi}\vec{\phi}(\vec{x}) + \Omega\vec{\chi}(\vec{x}) + \vec{f}(\vec{x},t) + \vec{f}_b(\vec{x},t) - \frac{i\hbar}{2\tau_\phi}\vec{\phi}(\vec{x}). \quad (2)$$

In previous work these equations were used to study the scattering of polaritons by a single impurity [16], the spatial structure formed by microcavity parametric oscillator polaritons [17], and the dispersion of polariton superfluids [18]. m_χ and m_ϕ are effective masses assigned to the parabolic dispersions of excitons and cavity photons with respect to the in-plane wave vector. Ω is the exciton-photon coupling constant [10,19]. V_0 and V_1 are constants determining the strength of the nonlinear interactions [18,20]. τ_χ and τ_ϕ are the lifetimes of excitons and photons, which account for the inelastic scattering and radiative decay of polaritons. $f(\vec{x},t)$ represents an optical pumping, which for two coherent, counterpropagating, continuous wave, Gaussian pumps is given by the Fourier integral:

$$\vec{f}(\vec{x},t) = \begin{pmatrix} A_x \\ A_y \end{pmatrix}\iint e^{-iE_pt/\hbar}\frac{i\Gamma}{[E_{\mathrm{LP}}(\vec{k}) - E_p - i\Gamma)]} \times (e^{-L^2(\vec{k}-\vec{k}_p)^2/4} + e^{-L^2(\vec{k}+\vec{k}_p)^2/4})d\vec{k}, \quad (3)$$

where A_x and A_y define the amplitudes of the two linearly polarized components of the pump. E_p is the pump energy, $\vec{k}_p$ and $-\vec{k}_p$ are the pump in-plane wave vectors, and L defines the width of each laser spot in real space. The fraction $\Gamma/[E_{\mathrm{LP}}(\vec{k}) - E_p - i\Gamma)]$ accounts for the nonuniform optical absorption [21]. $E_{\mathrm{LP}}(\vec{k})$ is the bare dispersion of the lower polariton branch. $\vec{f}_b(\vec{x},t)$ is a Langevin noise term much smaller in magnitude ($\times 10^{-4}$) than the pump. We take this term as a random white noise with no correlation between each point in space and time. This term includes the vacuum quantum noise and the noise due to Rayleigh scattering.

Equations (1) and (2) completely determine the dynamics of interacting polaritons once initial wave functions and parameters are defined.

Experimental setup.—The experimental setup is shown in Fig. 2. The laser source is a cw Ti:Sa laser, intensity stabilized, with a 1 MHz linewidth. The microcavity sample is cooled at 4 K in a cold finger cryostat. The sample is described in detail in Ref. [22]. It is a high quality factor 2λ GaAs/AlAs cavity, with three low indium content $In_{0.04}Ga_{0.96}As$ quantum wells, one at each antinode of the cavity mode. The Rabi splitting energy is 5.1 meV. Polariton linewidths are in the 100 μeV range, corresponding to a lifetime, τ, in the 10 ps range. The pump beams are resonant with the lower polariton branch at the same energy but with opposite in-plane wave vectors $\vec{k}_p$, $-\vec{k}_p$. The angle of incidence is about 3°. The spots of the two pump lasers are superimposed and have a size of about 40 μm. The two pump beams are linearly polarized, and the linear polarization of one of the pumps can be continuously and independently changed from a horizontal linear polarization to a vertical linear polarization with a half-wave plate. The light emitted by the microcavity is first collimated with a high aperture ocular and a 50 mm lens. The far field image is then polarized and divided into two parts with a beam splitter. One part is directly recorded on a 1024×1024 CCD camera. The other part can be sent through a lens to give the near field contribution.

Polarization-controlled optical gates.—Our theoretical results are obtained from numerical solution of Eqs. (1) and (2) using an Adams-Bashforth-Moulton method [23]. The wave functions were initially set to zero at all points in

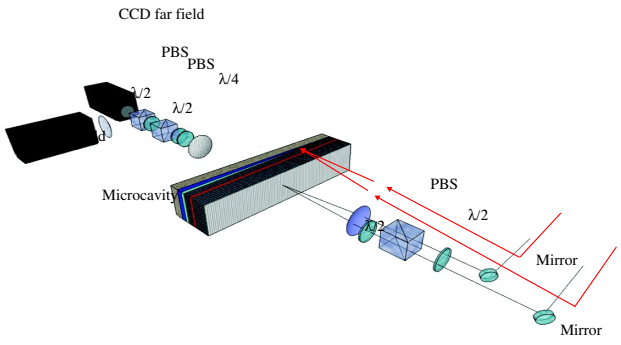

FIG. 2 (color online). Experimental setup. Two pump beams with equal energy and opposite in-plane wave vectors, $\vec{k}_p$ and $-\vec{k}_p$, are focused on the microcavity. The first pump is always horizontally linearly polarized (x). The linear polarization of the second pump can be continuously changed from a horizontal (x) to a vertical (y) polarization with a half-wave plate. The far field and near field emissions are analyzed with a polarization resolved setup and imaged on a CCD camera.

space. In Figs. 3 and 4 the theoretical results are compared with experimental images obtained at a pump intensity of 40 mW, in the cases of co- and cross-polarized pumps, respectively. When the two pumps are collinearly polarized, there is strong scattering to the wave vectors perpendicular to the pumps (accompanied by a change of linear polarization). We interpret this as an interference effect. For the scattering of a pair of polaritons from the quantum states i and j into the quantum states m and n there exist multiple channels. In particular, the polariton i can scatter into the state m or into the state n, while the polariton j scatters into the state n or m, respectively. These two processes have different amplitudes, in general, which may cause both constructive and destructive interference. In the particular case of scattering to $+90°$ and $-90°$ their amplitudes coincide because of the symmetry of the two scattering paths. This causes constructive interference, which makes the scattering at right angles preferential for polaritons with identical linear polarizations. The detailed microscopic theory of polariton-polariton scattering requires accounting for various exchange mechanisms (i.e. hole, electron, and photon exchanges) and is quite complicated. To our knowledge, it has been constructed only for the polarizationless case [24]. We note that the direction of preferential scattering in our experiments is also affected by the crystal anisotropy. A detailed study of the effect of crystal anisotropy on the spatial distribution of emission will be published elsewhere.

Qualitatively, the suppression of scattering in the case of cross-linearly polarized pumps can be inferred from the symmetry of the polariton pseudospin vector (Fig. 5). The pseudospin vector is the quantum analogue of the Stokes vector; its components are given by

$$S_x = \frac{|\phi_x|^2 - |\phi_y|^2}{S_0}, \qquad S_y = \frac{\phi_x^* \phi_y + \phi_y^* \phi_x}{S_0},$$
$$S_z = i\frac{\phi_x^* \phi_y - \phi_y^* \phi_x}{S_0}, \qquad S_0 = |\phi_x|^2 + |\phi_y|^2.$$

In the case of copolarized pumps, we observe stronger scattering to the cross-polarized states (inversion of pseudospin). This is a consequence of the difference in sign between polariton-polariton interaction constants in singlet and triplet configurations as discussed in Refs. [15,20]. Figure 5(b) shows that in the case of cross-polarized pumps there can be no preferential direction of the pseudospin of the signal states. From this we should expect the suppression of scattering to the signal states. We stress that this effect is not linked to the difference of interaction constants and persists at any value of α_2.

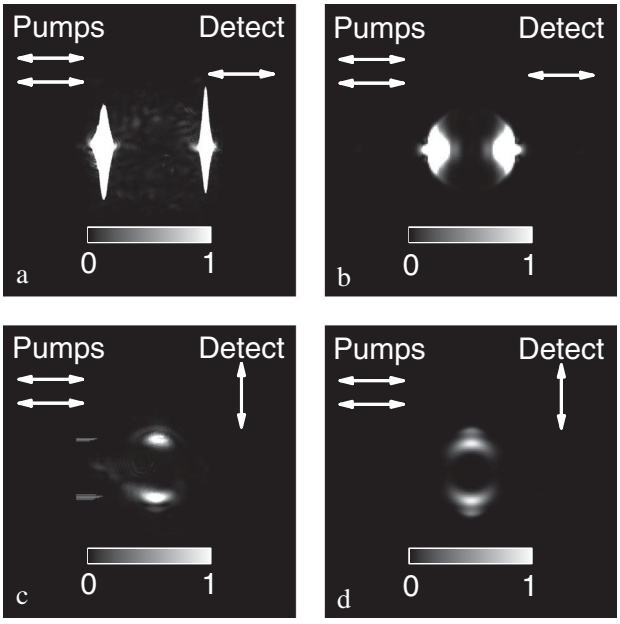

FIG. 3. Far field images in the case of collinear, horizontally (x) polarized pump beams. (a) Experimentally measured horizontally (x) polarized intensity. The CCD is deliberately saturated in order to detect any weak emission along the vertical axis. (b) Theoretically calculated horizontally (x) polarized intensity, obtained from a time integrated Fourier transform of $\vec{\phi}(\vec{x})$. (c) Experimentally measured vertically (y) polarized intensity. (d) Theoretically calculated vertically (y) polarized intensity. The intensity scale in (b) is saturated so that it is the same as the one (d); the maximum intensity in (b) is actually $\times 400$ larger than that in (d). Parameters used in theory: $m_\chi = 0.22 m_e$, $m_\phi = 10^{-5} m_e$ (m_e is the free electron mass), $\Omega = 2.55$ meV, $|\vec{k}_p| = 390\ \mathrm{mm}^{-1}$, $V_0 = 1 \times 10^{-6}$ meV mm^2, $V_1 = 0.55 V_0$, $\tau_\chi = 100$ ps, $\tau_\phi = 4.7$ ps, $|A_x, A_y| = 160$ meV mm^{-1}, $\Gamma = 0.2$ meV, $L = 34\ \mu$m, $E_p = E_{\mathrm{LP}}(\vec{k}_p) + 0.05$ meV.

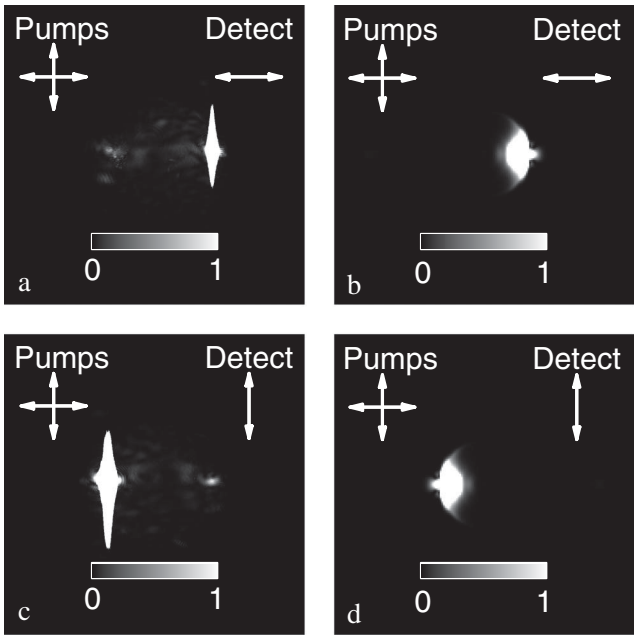

FIG. 4. Far field images in the case of cross-linearly (x and y) polarized pumps. (a) and (c) show the experimentally measured intensity in the x and y polarizations. (b) and (d) show the corresponding results from theory. All intensity scales are saturated to detect any weak scattering.

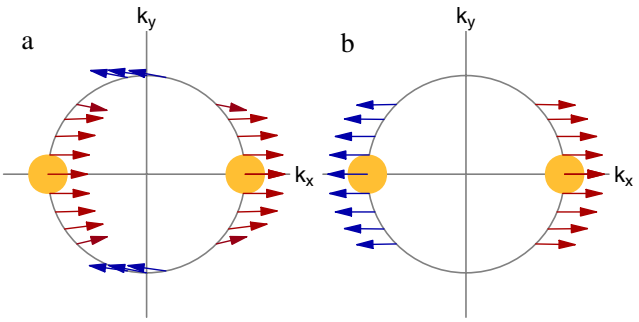

FIG. 5 (color online). The variation of the (time-averaged) pseudospin vector, (S_x, S_y, S_z), around a circle in reciprocal space with radius equal to the pump wave vector, obtained from the numerical solution of Eqs. (1) and (2). (a) Copolarized pumps; (b) cross-polarized pumps.

We note that our device functions as an all-optical XNOR (exclusive-NOR) logic gate, that is, a binary logic gate that outputs "true" if its two inputs are the same and outputs "false" if its two inputs are different. All-optical XNOR gates are critical in several applications, including: optical packet address recognition, data comparison, optical generation of pseudorandom patterns, and encryption. Existing designs of optical XNOR gates, based on semiconductor micro-ring resonators [25] and semiconductor optical amplifiers [26,27], tend to rely on the linking of more than one individual elements or gates. The inclusion of the whole gate in one element, a semiconductor microcavity, could allow the construction of optical circuits on smaller length scales.

Note that in our model we have ignored the longitudinal-transverse (LT) splitting of polaritons as it is not significant in our experiment. In fact, the LT splitting allows exact energy-momentum conservation for the process demonstrated in Fig. 1(a), if accompanied by the rotation of linear polarization that we have observed. However, at intermediate scattering angles (not equal to 90°), the LT splitting could lead to the appearance of circular polarizations as in the optical spin Hall effect (OSHE) [28]. Polarization conversion due to the LT splitting is a linear optical effect, independent of the pumping intensity, unlike the polariton-polariton scattering discussed in this Letter. By varying the pump intensity one can switch between the OSHE and the present effect.

In the experiment our optical gate requires a threshold power of 9 mW ($\sim$1 kW/cm^2 for our spot size). The response time obtained numerically is about 1000 ps. This value is sensitive to the spontaneous scattering (with disorder and phonons) that provides an initial seed for the nonlinear scattering processes. It is likely that the response time can be improved by altering the disorder and temperature in the microcavity.

Conclusion.—The degenerate polariton parametric scattering between two pumps is strongly influenced by their relative polarization. In the case of copolarized pumps there is strong scattering, while in the case of cross-polarized pumps there is no such effect. The observed effect is a manifestation of the interference between coherent polariton fields. This allows a semiconductor microcavity to function as a polarization-controlled solid-state optical gate, as we have demonstrated.

I. A. S. acknowledges support from a grant of the president of the Russian Federation. T. C. H. L. acknowledges the EPSRC.

[1] M. M. Salour and C. Cohen-Tannoudji, Phys. Rev. Lett. **38**, 757 (1977).
[2] A. Barenco, D. Deutsch, A. Ekert, and R. Jozsa, Phys. Rev. Lett. **74**, 4083 (1995).
[3] A. P. Heberle, J. J. Baumberg, and K. Köhler, Phys. Rev. Lett. **75**, 2598 (1995).
[4] J. Kasprzak *et al.*, Nature (London) **443**, 409 (2006).
[5] H. W. Tan *et al.*, Phys. Rev. B **70**, 205110 (2004).
[6] V. Van *et al.*, IEEE Photonics Technol. Lett. **14**, 74 (2002).
[7] T. A. Ibrahim *et al.*, IEEE Photonics Technol. Lett. **15**, 36 (2003).
[8] V. R. Almeida, C. A. Barrios, R. R. Panepucci, and M. Lipson, Nature (London) **431**, 1081 (2004).
[9] C. Weisbuch, M. Nishioka, A. Ishikawa, and Y. Arakawa, Phys. Rev. Lett. **69**, 3314 (1992).
[10] A. V. Kavokin and G. Malpuech, *Cavity Polaritons* (Elsevier, New York, 2003).
[11] P. G. Savvidis *et al.*, Phys. Rev. Lett. **84**, 1547 (2000).
[12] M. Saba *et al.*, Nature (London) **414**, 731 (2001).
[13] M. Romanelli, C. Leyder, J. Ph. Karr, E. Giacobino, and A. Bramati, Phys. Rev. Lett. **98**, 106401 (2007).
[14] S. Savasta, O. Di Stefano, V. Savona, and W. Langbein, Phys. Rev. Lett. **94**, 246401 (2005).
[15] I. A. Shelykh, A. V. Kavokin, and G. Malpuech, Phys. Status Solidi (b) **242**, 2271 (2005).
[16] I. Carusotto and C. Ciuti, Phys. Rev. Lett. **93**, 166401 (2004).
[17] D. M. Whittaker, Phys. Status Solidi (c) **2**, 733 (2005).
[18] I. A. Shelykh *et al.*, Phys. Rev. Lett. **97**, 066402 (2006).
[19] G. Panzarini *et al.*, Phys. Rev. B **59**, 5082 (1999).
[20] P. Renucci *et al.*, Phys. Rev. B **72**, 075317 (2005).
[21] H. Haug and S. W. Koch, *Quantum Theory of the Optical and Electronic Properties of Semiconductors* (World Scientific, Singapore, 1994).
[22] R. Houdré *et al.*, Phys. Rev. B **61**, R13333 (2000).
[23] D. R. Kincaid and E. W. Cheney, *Numerical Analysis* (Brooks Cole, Belmont, MA, 1991).
[24] M. Combescot, M. A. Dupertuis, and O. Betbeder-Matibet, Europhys. Lett. **79**, 17001 (2007).
[25] V. Van *et al.*, IEEE J. Sel. Top. Quantum Electron. **8**, 705 (2002).
[26] S. Lee *et al.*, Jpn. J. Appl. Phys. **41**, L1155 (2002).
[27] S. Kumar and A. E. Willner, Opt. Express **14**, 5092 (2006).
[28] A. V. Kavokin, G. Malpuech, and M. M. Glazov, Phys. Rev. Lett. **95**, 136601 (2005).